Intermediate-Temperature Superfluidity in an Atomic Fermi Gas with Population Imbalance

Chih-Chun Chien, Qijin Chen, Yan He, and K. Levin

James Franck Institute and Department of Physics, University of Chicago, Chicago, Illinois 60637, USA

(Received 1 May 2006; published 1 September 2006)

We derive the underlying finite temperature theory which describes Fermi gas superfluidity with population imbalance in a homogeneous system. We compute the pair formation temperature, superfluid transition temperature T_c, and superfluid density in a manner consistent with the standard ground state equations and, thereby, present a complete phase diagram. Finite temperature stabilizes superfluidity, as manifested by two solutions for T_c or by low T instabilities. At unitarity, the polarized state is an ''intermediate-temperature superfluid.''

DOI: 10.1103/PhysRevLett.97.090402 PACS numbers: 05.30.Fk, 03.75.Hh, 03.75.Ss, 74.20.−z

Excitement in the field of ultracold Fermi gases has to do with their remarkable tunability. As a magnetic field is varied from weak to strong, this system undergoes a transition from a Bose Einstein condensate (BEC) to a BCS-based superfluid. Recently [1,2], another tunability has emerged; one can vary the population imbalance between the two ''spin'' species. This capability has led to speculations about new phases of superfluidity, quantum critical points, and has repercussions as well in other subfields of physics [3,4]. A nice body of theoretical work on this subject [5–8] has focused on zero temperature (T) studies of the simplest mean-field wave function [9], with population imbalance. Additional important work presents [10] a $T = 0$ two-channel, mean-field approach for very narrow Feshbach resonances, as well as a study of finite T effects [11], albeit without a determination of superfluid order.

Superfluidity is, generally, a finite T phenomenon, and it is the purpose of the present Letter to explore finite temperature effects [12–14] based on the BCS-Leggett ground state with population imbalance. We determine the behavior of the pair formation temperature T^*, the superfluid transition temperature T_c, and superfluid density $n_s(T)$ and, thereby, arrive at a phase diagram which addresses general T. Importantly, we find that in the fermionic regime, superfluidity exists at finite T (although not at $T = 0$), leading to the new concept of an ''intermediate-temperature superfluid.'' Because temperature acts in this rather unexpected fashion, we reduce the complexity and confine our attention to the homogeneous system.

The approach which we outline below, importantly, includes what we call ''pseudogap effects.'' For $T \neq 0$, the excitation gap Δ is different from the order parameter, due to the contribution to Δ from *noncondensed pairs* [12,15]. In this way, the solution for T_c is necessarily different from that obtained in the literature. Generally, Δ^2 contains two additive contributions [13,14] from the condensate (Δ^2_{sc}) and noncondensed pairs (Δ^2_{pg}), and they are proportional to the total, condensed, and noncondensed pair densities, respectively. This decomposition is analogous to the particle number constraint in ideal BEC. We emphasize that the central equations derived below are *not* compatible [15] with the $T \neq 0$ formalism of Ref. [16]. In addition, the ''naive mean-field theory'' with the unphysical assumption that $\Delta(T) \equiv \Delta_{sc}(T)$ is not a correct rendition of $T \neq 0$ effects associated with the BCS-Leggett ground state.

We define the noncondensed pair propagator, as $t(Q) = U/[1 + U\chi(Q)]$, where, as in Ref. [14], the pair susceptibility, given by $\chi(Q) = \frac{1}{2}\sum_K[G_{0\uparrow}(Q-K)G_\downarrow(K) + G_{0\downarrow}(Q-K)G_\uparrow(K)]$, can be derived from equations for the Green's functions, consistent with the BCS-Leggett ground state equations. Here $G_\sigma(K)$ and $G_{0,\sigma}(K) = i\omega_n - \xi_{\mathbf{k},\sigma}$ are the full and bare Green's functions, respectively (with $\sigma = \uparrow, \downarrow$, $\xi_{\mathbf{k},\sigma} = \epsilon_{\mathbf{k}} - \mu_\sigma$). We adopt a one-channel approach, since the ^{6}Li resonances studied thus far are broad, and consider a Fermi gas of two spin species with kinetic energy $\epsilon_{\mathbf{k}} = \hbar^2k^2/2m$ and chemical potential $\mu_\uparrow$ and $\mu_\downarrow$, subject to an attractive contact potential ($U < 0$) between the different spin states. We take $\hbar = 1$, $k_B = 1$, and $K \equiv (i\omega_n, \mathbf{k})$, $Q \equiv (i\Omega_n, \mathbf{q})$, $\sum_K \equiv T\sum_n\sum_{\mathbf{k}}$, etc., where ω_n (Ω_n) is the standard odd (even) Matsubara frequency.

In the superfluid state, the ''gap equation'' is given by $U^{-1} + \chi(0) = 0$, which is equivalent to $\mu_{pair} = 0$, the BEC condition of the pairs. Below T_c, the self-energy can be well approximated [12] by the BCS form $\Sigma_\sigma(K) = -\Delta^2 G_{0,\bar\sigma}(-K)$, where $\bar\sigma = -\sigma$. Therefore, $G_{\uparrow,\downarrow}(K) = u^2_{\mathbf{k}}/(i\omega_n \pm h - E_{\mathbf{k}}) + v^2_{\mathbf{k}}/(i\omega_n \pm h + E_{\mathbf{k}})$, where $E_{\mathbf{k}} = \sqrt{\xi^2_{\mathbf{k}} + \Delta^2}$, $\xi_{\mathbf{k}} = \epsilon_{\mathbf{k}} - \mu$, $\mu = (\mu_\uparrow + \mu_\downarrow)/2$, $h = (\mu_\uparrow - \mu_\downarrow)/2$, and $u^2_{\mathbf{k}}, v^2_{\mathbf{k}} = (1 \pm \xi_{\mathbf{k}}/E_{\mathbf{k}})/2$. Since the polarization $p > 0$, we always have $h > 0$.

The gap equation can then be rewritten in terms of the two-body s-wave scattering length a leading to

$$\frac{m}{4\pi a} = \sum_{\mathbf{k}}\left[\frac{1}{2\epsilon_{\mathbf{k}}} - \frac{1 - 2\bar f(E_{\mathbf{k}})}{E_{\mathbf{k}}}\right], \tag{1}$$

where $\bar f(x) \equiv [f(x+h) + f(x-h)]/2$, and $m/4\pi a = 1/U + \sum_{\mathbf{k}}(2\epsilon_{\mathbf{k}})^{-1}$. Here $f(x)$ is the Fermi distribution function. We define $pn \equiv \delta n = n_\uparrow - n_\downarrow > 0$, where $n = n_\uparrow + n_\downarrow$ is the total atomic density, and $p = \delta n/n$. Similarly, using $n_\sigma = \sum_K G_\sigma(K)$, one can write

$$n = 2\sum_{\mathbf{k}}\left[v_{\mathbf{k}}^2 + \frac{\xi_{\mathbf{k}}}{E_{\mathbf{k}}}\bar{f}(E_{\mathbf{k}})\right], \tag{2a}$$

$$pn = \sum_{\mathbf{k}}[f(E_{\mathbf{k}} - h) - f(E_{\mathbf{k}} + h)]. \tag{2b}$$

Note that, except for the number difference [Eq. (2b)], all equations including those below can be obtained from their unpolarized counterparts by replacing $f(x)$ and its derivative $f'(x)$ with $\bar{f}(x)$ and $\bar{f}'(x)$, respectively.

While Eqs. (1) and (2) have been written down in the literature [5,11], the present derivation can be used to go further and to determine the dispersion relation and the number density for noncondensed pairs. We find

$$\Delta_{\text{pg}}^2 \equiv -\sum_{Q\neq 0} t(Q), \tag{3}$$

which vanishes at $T = 0$, where $\Delta^2 = \Delta_{\text{sc}}^2$. In the superfluid phase, $t^{-1}(Q) = \chi(Q) - \chi(0) \approx Z(\Omega - \Omega_{\mathbf{q}})$ to first order in Ω and after analytical continuation ($i\Omega_n \to \Omega + i0^+$). Here $\chi(Q) = \sum_{\mathbf{k}}\{[1 - \bar{f}(E_{\mathbf{k}}) - \bar{f}(\xi_{q-k})]/(E_{\mathbf{k}} + \xi_{\mathbf{q-k}} - i\Omega_n)u_{\mathbf{k}}^2 - [\bar{f}(E_{\mathbf{k}}) - \bar{f}(\xi_{q-k})]/(E_{\mathbf{k}} - \xi_{q-k} + i\Omega_n)v_{\mathbf{k}}^2\}$. It follows that the inverse residue $Z = [n - 2\sum_{\mathbf{k}}\bar{f}(\xi_{\mathbf{k}})]/2\Delta^2$. Thus, $\Delta_{\text{pg}}^2 = Z^{-1}\sum_{\mathbf{q}} b(\Omega_{\mathbf{q}})$, where $b(x)$ is the Bose distribution function. To lowest order in $\mathbf{q}$, the pair dispersion $\Omega_{\mathbf{q}} = q^2/2M^*$, where the effective pair mass M^* can be computed from a low q expansion of $\Omega_{\mathbf{q}}$. This q^2 dispersion is associated [12] with BCS-type ground states, which have been the basis for essentially all population imbalance work.

Importantly, Eqs. (1)–(3) can be used to determine T_c as the extremal temperature(s) in the normal state at which noncondensed pairs exhaust the total weight of Δ^2 so that $\Delta_{\text{pg}}^2 = \Delta^2$. Solving for the "transition temperature" in the absence of pseudogap effects leads to the quantity T_c^{MF}. More precisely, T_c^{MF} is defined to be the temperature at which $\Delta(T)$ vanishes within Eqs. (1) and (2). This provides a reasonable estimate for the pairing onset temperature T^*, when a stable superfluid phase exists. It should be noted that T^* represents a smooth crossover rather than an abrupt phase transition and that Eq. (1) must be altered [17] above T_c to include finite μ_{pair}. We will see that understanding the behavior of T_c^{MF} is a necessary first step en route to understanding the behavior of T_c itself.

The superfluid density $n_s(T)$ is also required to vanish at the same value(s) for T_c, as deduced above. Our calculation of n_s closely follows previous work [14,18] for the case of the unpolarized superfluid. There is an important cancellation between the current vertex and self-energy contributions involving Δ_{pg}^2 so that, as expected, $n_s(T)$ varies with the order parameter Δ_{sc}^2. It is given by

$$n_s(T) = \frac{4}{3}\Delta_{\text{sc}}^2\sum_{\mathbf{k}}\frac{\epsilon_{\mathbf{k}}}{E_{\mathbf{k}}^2}\left[\frac{1 - 2\bar{f}(E_{\mathbf{k}})}{2E_{\mathbf{k}}} + \bar{f}'(E_{\mathbf{k}})\right], \tag{4}$$

which at $T = 0$ agrees with Ref. [5].

The stability requirements for the superfluid phase have been discussed in the literature [5]. In general, one requires that the superfluid density be positive and that the 2×2 "number susceptibility" matrix for $\partial n_\sigma/\partial\mu_{\sigma'}$ have only positive eigenvalues when the gap equation is satisfied. The Δ dependence of n_σ introduces into the matrix the overall factor $(\partial^2\Omega/\partial\Delta^2)_{\mu,h}^{-1}$. Thus, the second stability requirement is equivalent to the condition that

$$\left(\frac{\partial^2\Omega}{\partial\Delta^2}\right)_{\mu,h} = 2\sum_{\mathbf{k}}\frac{\Delta^2}{E_{\mathbf{k}}^2}\left[\frac{1 - 2\bar{f}(E_{\mathbf{k}})}{2E_{\mathbf{k}}} + \bar{f}'(E_{\mathbf{k}})\right] > 0. \tag{5}$$

Here Ω is the thermodynamical potential. A third stability requirement, specific to the present calculations, is that the pair mass $M^* > 0$.

In Fig. 1, we present a plot of T_c^{MF} as a function of $1/k_Fa$ for a range of p. In the inset, we plot $\Delta(T)$ at different $1/k_Fa$ for $p = 0.3$. For $p < 0.9$ and sufficiently low T_c^{MF}, the curves for T_c^{MF} develop an unexpected structure, as one sweeps toward the BCS regime. Once $1/k_Fa$ is less than a critical value, $(1/k_Fa)_c$ where T_c^{MF} vanishes, there are two T_c^{MF} lines. The lower branch starts from $(1/k_Fa)_c$ and increases as $1/k_Fa$ decreases. This structure implies that Δ is nonmonotonic [19] in T, as indicated by the bottom curve in the inset in Fig. 1. The two zeros of Δ represent the two values of T_c^{MF}. In contrast to the more conventional behavior (shown in the top curve for a stronger pairing interaction), Δ *increases* with T at low temperature when $1/k_Fa$ is sufficiently small. This indicates that *temperature enables pairing*. This was also inferred in Ref. [11]. In general superfluids, one would argue that these two effects compete.

Insight into this important phenomenon in the fermionic regime ($\mu > 0$) is provided by studying the momentum distribution $n_\sigma(k)$ at $T = 0$ and finite T. At $T = 0$, pairing is present only for $\epsilon_{\mathbf{k}}$ below $\epsilon_1 = \max(0, \mu - \sqrt{h^2 - \Delta^2})$ and above $\epsilon_2 = \mu + \sqrt{h^2 - \Delta^2}$. This polarized $T = 0$ state requires that pairs persist to relatively high energies

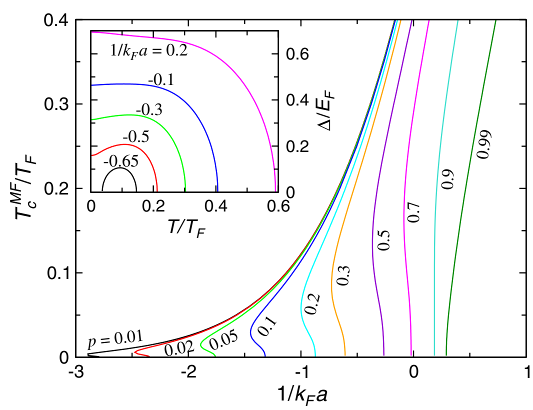

FIG. 1 (color online). Mean-field behavior of T_c^{MF} as a function of $1/k_Fa$ for different p. Shown in the inset is the pairing gap $\Delta(T)$ at different $1/k_Fa$ for $p = 0.3$. Here $E_F \equiv k_BT_F \equiv \hbar^2k_F^2/2m$ is the noninteracting Fermi energy for $p = 0$.

$\epsilon_{\mathbf{k}} > \epsilon_2$, as a result of the Pauli principle which pushes these states out of the "normal" regime occupied by the majority species. This kinetic energy cost competes with the gain from condensation energy, and, for a sufficiently weak attraction, this "breached pair" structure [20] becomes unstable at $T = 0$. By contrast, at finite T the regime originally occupied exclusively by the majority species between ϵ_1 and ϵ_2 is no longer completely filled, and pairs can "spill over" from both lower and higher energy states into this regime. This not only helps lower the kinetic energy but allows the normal regime to participate in pairing and, thus, lowers the potential energy. In this way, temperature can enhance pairing. It should be noted that the majority species between ϵ_1 and ϵ_2 contains a pairing self-energy and is different from a free Fermi gas.

Figure 2 represents solutions for T_c of our central equation set [Eqs. (1)–(3)] as a function of $1/k_F a$ for the entire range of p. If the solution for T_c falls into the shaded region, there is no stable superfluid [since $\partial^2\Omega/\partial\Delta^2 < 0$, through Eq. (5)]. For low polarizations $p \lesssim 0.185$, the behavior of T_c is similar to that of $T_c^{\rm MF}$ when one approaches the BCS regime. There may be one or two T_c's which, when stable, will be associated with intermediate-temperature superfluidity. When $p > 0.185$, however, no solution can be found for the regime $1/k_F a \lesssim 0.18$, because $M^* < 0$ there. We stress that *the origin of the intermediate-temperature superfluid we find here lies in a very early stage of the calculations*; it can already be seen as a consequence of the constraints imposed on the *pairing gap* in the low T regime when there is a delicate energetic balance between normal and paired states [see Eqs. (1) and (2) and Fig. 1].

In Fig. 3, we summarize our observations in the form of a general temperature phase diagram. In region I, the system is normal and superfluidity is absent. However, this normal phase need not be a Fermi gas. Close to the boundary, as shown in the inset in Fig. 1 (bottom curve), finite T pairing may occur with or without phase coherence. In region III, stable superfluidity is present for all $T \le T_c$. Finally, in region II, within the shaded region (IIC and IID), we find a stable polarized superfluid phase for intermediate temperatures, not including $T = 0$, which we refer to as intermediate-temperature superfluidity. In IIA and IIB, no stable polarized superfluid is found. The nearly vertical line represents $T_c = 0$ around $1/k_F a \approx 0.18$, roughly independent of p (see Fig. 2).

Finite momentum condensates [10,21] may well occur in any of the regimes in II, particularly IIA and IIB, for which our equations do not yield stable zero momentum condensation. Future work will explore the nature of the stable phases in these regimes. The boundaries of the region denoted II can be compared with other $T = 0$ phase diagrams in the literature [5,10]. In contrast to Ref. [5], we find that the most stringent criterion for stability at $T = 0$ is the positivity of the second order partial derivative $\partial^2\Omega/\partial\Delta^2$ [as given in Eq. (5)]. This defines the boundary between II and III. This is substantially different from the line associated with $n_s(0) = 0$ (used in Ref. [5]) which is described by a nearly vertical line from $(p, 1/k_F a) = (1, 0.3)$ to $(0, 0.6)$. Similarly, the locus of points in the two-dimensional parameter space $(p, 1/k_F a)$ where $T_c^{\rm MF}$ vanishes defines the boundary between I and II, as is consistent with its counterpart in Ref. [5].

In region IID, we define $T_{\rm unstable}$ (which is below the single T_c) as the temperature where the system becomes unstable, via Eq. (5). At a given $1/k_F a$, $T_{\rm unstable}$ decreases with decreasing p and approaches 0 as $p \to 0$. This is

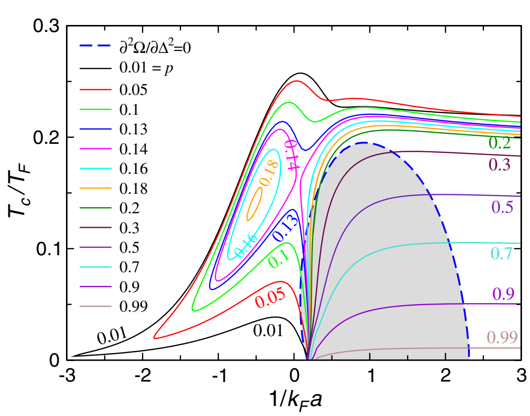

FIG. 2 (color online). T_c as a function of $1/k_F a$ for different p. The T_c curve splits into two disconnected curves for $0.14 \lesssim p \lesssim 0.185$. The T_c solution inside the shaded area is unstable.

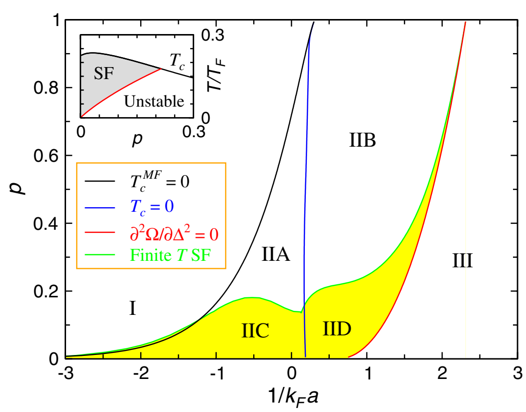

FIG. 3 (color online). Phase diagram on the $p - 1/k_F a$ plane with the nearly vertical line corresponding to $T_c = 0$. Yellow region (shaded) corresponds to intermediate-temperature superfluidity. Region I, the system is normal; IIA, $M^* < 0$ so no solution for T_c exists; IIB, solution for T_c exists but superfluid state is unstable; IIC, superfluid state exists at intermediate T between upper and lower T_c's but not $T = 0$; IID, superfluid state exists at finite T but becomes unstable at a low temperature $T_{\rm unstable}$ (shown in the inset for $1/k_F a = 0.5$) where n_s is finite; III, superfluid state exists for all $T \le T_c > 0$. The chemical potential μ changes sign within regions IIB and IID (close to $1/k_F a \approx 0.6$ for all p), while $n_s(0)$ vanishes along a nearly vertical line (not shown) between $(p, 1/k_F a) = (1, 0.3)$ and $(0, 0.6)$. The $p \equiv 0$ boundary is not continuously connected to the rest of the phase diagram.

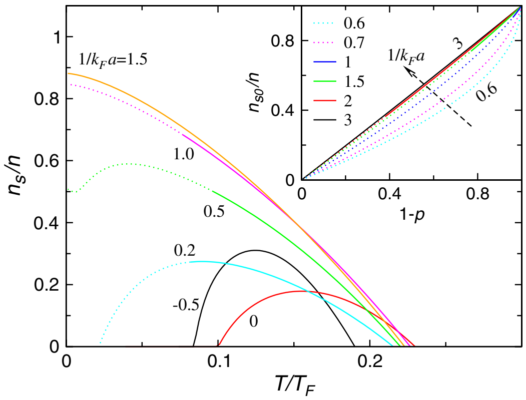

FIG. 4 (color online). Normalized superfluid density n_s/n as a function of T/T_F at $p = 0.1$ for various $1/k_F a$ from BCS to BEC, corresponding to regions IIC ($1/k_F a = -0.5$ and 0), IID (0.2, 0.5, 1.0), and III (1.5), respectively. The inset plots $n_{s0} \equiv n_s(T = 0)$ versus $1 - p$ for different $1/k_F a$, indicating $n_{s0} \to 2n_\downarrow$ in the BEC limit. The dotted (segments of the) curves represent unstable solutions within region IIB (IID).

shown in the inset in Fig. 3 for $1/k_F a = 0.5$. In region IIC, the lower T_c approaches 0 as p approaches 0. Thus, there is an important distinction between the $p \equiv 0$ and $p \to 0^+$ limits, especially at $T = 0$. For p small but finite, calculations readily encounter instabilities at strictly $T = 0$, and here superfluidity is very fragile to the introduction of small imbalance. By contrast, at finite T this fragility is not as pronounced. We conclude that only $T \equiv 0$ is a problematic temperature for weakly polarized superfluidity.

Figure 4 presents $n_s(T)$ for $p = 0.1$. Except for the case $1/k_F a = 1.5$, Fig. 4 shows the typical behavior in region II (of Fig. 3) corresponding to intermediate-temperature superfluidity. The observations here (and associated nonmonotonicities) for $n_s(T)$ are similar in many ways to what is seen for $\Delta(T)$ in the inset in Fig. 1. In region IIC, n_s goes to zero at the upper and lower T_c, whereas in IID, $n_s(T)$ abruptly stops at T_{unstable}. The dotted lines indicate that they are in the unstable regime. Throughout region III, n_s is found to be monotonically decreasing with increasing T, as in conventional superfluids. Finally, in the inset in Fig. 4, we plot $n_{s0} \equiv n_s(0)$ as a function of $1 - p = 2n_\downarrow/n$. Only in the deep BEC regime is the dependence linear. This plot reflects that the excess unpaired fermions interact with the paired states, leading to a reduced superfluid density at $T = 0$ relative to $2n_\downarrow$.

The experimental situation regarding the stability of a unitary polarized superfluid (UPS) is currently being unraveled [1,2]. If one includes the trap, within the local density approximation it appears [6,7,11] that the local polarization $p(r)$, in effect, increases continuously from a small value at the trap center to 100% at the trap edge. It follows from this Letter that at very low T the superfluid trap center will not support polarization, but, for a range of T closer to T_c, polarization can penetrate the core. We estimate from Fig. 2 (assuming the central $p \sim 0.05$) that there exists a UPS for $T \sim 0.05$–$0.25T_F$. Given the temperature range in experiment [1], this appears to be not inconsistent with current data [$T_F = 1.9\ \mu$K, $T = 300$–505 nK $= (0.16$–$0.27)T_F$ on resonance]. In the near-BEC regime, our predictions also appear consistent with new data in Ref. [22]. More generally, because the local $p(r = 0)$ is small and the unstable region is suppressed to very low T as $p \to 0$, this may explain why superfluidity in atomic traps can be observed experimentally. Future theory including the trap will be required to provide quantitative comparison with experiment.

This work was supported by NSF-MRSEC Grant No. DMR-0213745, and we thank C. Chin, W. Yi, M. W. Zwierlein, and R. G. Hulet for useful communications.

[1] M. W. Zwierlein, A. Schirotzek, C. H. Schunck, and W. Ketterle, Science **311**, 492 (2006).
[2] G. B. Partridge, W. Li, R. I. Kamar, Y. A. Liao, and R. G. Hulet, Science **311**, 503 (2006).
[3] W. V. Liu and F. Wilczek, Phys. Rev. Lett. **90**, 047002 (2003).
[4] M. M. Forbes, E. Gubankova, W. V. Liu, and F. Wilczek, Phys. Rev. Lett. **94**, 017001 (2005).
[5] C. H. Pao, S. T. Wu, and S. K. Yip, Phys. Rev. B **73**, 132506 (2006).
[6] T. N. De Silva and E. J. Mueller, Phys. Rev. A **73**, 051602(R) (2006).
[7] M. Haque and H. T. C. Stoof, cond-mat/0601321.
[8] P. Pieri and G. C. Strinati, Phys. Rev. Lett. **96**, 150404 (2006).
[9] A. J. Leggett, in *Modern Trends in the Theory of Condensed Matter* (Springer-Verlag, Berlin, 1980), pp. 13–27.
[10] D. Sheehy and L. Radzihovsky, Phys. Rev. Lett. **96**, 060401 (2006).
[11] W. Yi and L. M. Duan, Phys. Rev. A **73**, 031604(R) (2006).
[12] Q. J. Chen, J. Stajic, S. N. Tan, and K. Levin, Phys. Rep. **412**, 1 (2005).
[13] I. Kosztin, Q. J. Chen, B. Jankó, and K. Levin, Phys. Rev. B **58**, R5936 (1998).
[14] Q. J. Chen, I. Kosztin, B. Jankó, and K. Levin, Phys. Rev. Lett. **81**, 4708 (1998).
[15] P. Pieri and G. C. Strinati, Phys. Rev. B **71**, 094520 (2005).
[16] P. Nozières and S. Schmitt-Rink, J. Low Temp. Phys. **59**, 195 (1985).
[17] Q. J. Chen, J. Stajic, and K. Levin, Phys. Rev. Lett. **95**, 260405 (2005).
[18] J. Stajic, A. Iyengar, Q. J. Chen, and K. Levin, Phys. Rev. B **68**, 174517 (2003).
[19] A. Sedrakian and U. Lombardo, Phys. Rev. Lett. **84**, 602 (2000).
[20] G. Sarma, J. Phys. Chem. Solids **24**, 1029 (1963).
[21] T. Mizushima, K. Machida, and M. Ichioka, Phys. Rev. Lett. **94**, 060404 (2005).
[22] M. W. Zwierlein, C. H. Schunck, A. Schirotzek, and W. Ketterle, Nature (London) **442**, 54 (2006).